Diffusion in Pore Networks: Effective Medium Theory and Smooth Field Approximation

The problem of diffusion in pore networks of a certain class is considered, and a procedure for estimating effective diffusivities is formulated. The effective-medium theory is used to obtain an effective conductance for the network, which is then used to determine the effective diffusivity starting from first physical principles and utilizing the observation that a network of pores of uniform conductance satisfies the smooth field approximation. Comparison of the estimated intraparticle diffusivities with those obtained from the exact solution of the transport equation for large networks reveals high accuracy and reliability of the method. Results for a number of pore networks show that the smooth field assumption should not be employed arbitrarily since it always predicts higher effective diffusion coefficients than the exact ones, by more than one order of magnitude in some cases.

V. N. Burganos, S. V. Sotirchos
Department of Chemical Engineering
University of Rochester
Rochester, NY 14627

Introduction

Mass transport in porous media plays a major role in gas-solid reactions, both catalytic and noncatalytic, involving particles or pellets of porous solids. Most of the industrially important gas-solid reactions occur in the transition regime of intraparticle diffusion and reaction, that is, under reaction conditions where both intrinsic kinetics and intraparticle diffusion are important. When mathematical models that describe the transient or steady state behavior of the above reactive systems are formulated for use in gas-solid reactor design or analysis of experimental reactivity data, appropriate expressions that relate the fluxes of the diffusing gaseous species in the porous structure to their concentrations and to the properties of the porous solid are needed in addition to material and energy balances. The effects of intraparticle mass transport limitations are usually more profound in noncatalytic gas-solid systems owing to the fact that the pore structure of the solid evolves locally and in time, leading in turn to changes in the resistance for mass transport in the porous medium. Recent computer simulation results by Sotirchos and Burganos (1986), for instance, have shown that the ignition and extinction phenomena observed in the combustion of coal-derived char particles are strongly influenced by the initial rate limitations for mass transport, as quantified by the effective diffusion coefficient, and their evolution with the progress of the reaction. Similar conclusions have been reached by Sotirchos and Yu (1985) for gas-solid reactions with solid product. It was found that the transient behavior of reacting calcined limestone particles in an environment of SO_2, and eventually their sorptive capacity for SO_2 removal from coal combustion gases, may depend more strongly on the intraparticle diffusivity than on the diffusion coefficient in the product layer.

Flux relations are usually the fruit of combined theoretical and experimental investigation of the intraparticle mass transport problem. Two are the most frequently used approaches in modeling the pore space of a given solid with the objective of deriving flux expressions (Jackson, 1977): the pore structure is treated as a capillary network, usually of cylindrical pores, or attention is focused on the way in which the solid phase obstructs the motion of the molecules in the gas phase. The latter approach is characteristic of the dusty-gas model (Mason et al., 1967; Mason and Malinauskas, 1983) and of related flux models.

Several flux models based on pore models of varying complexity have been presented in the literature (van Brakel, 1975; Jackson, 1977; Cunningham and Williams, 1980). However, most of these pore models consider special types of pore size distribution (discrete unimodal or bimodal, for instance), and con-

Correspondence concerning this paper should be addressed to S. V. Sotirchos.

sequently the applicability of the corresponding flux relations is rather limited. A general class of flux models that can be used with any type of pore size distribution was formulated by Stewart and coworkers (Johnson and Stewart, 1965; Feng and Stewart, 1973). For multicomponent mixtures, the dusty-gas model flux relations are used to describe diffusion in a single pore, and the flux relations for the porous medium are obtained by averaging over the pore size and pore orientation distributions.

A common feature of most pore-based flux models is that they consider that the smooth field assumption (Jackson, 1977) is valid, that is, that the axial concentration gradient in a pore segment is equal to the component of the macroscopic concentration gradient in the direction of the pore axis. The macroscopic concentration field is assumed to be a smooth function of position in the porous medium. The smooth field approximation clearly ignores the interaction of fluxes at the intersections of different capillaries, and hence it may violate the material balance equations there. As a result, the smooth field assumption holds rigorously only for networks of infinitely long, straight, nonoverlapping capillaries and, as we will see later, for some special types of networks. If the smooth field approximation is not used, the microscopic concentration field that is needed for the computation of the fluxes in the various pore segments can be obtained only by direct solution of the transport equation in the pore network. Such an approach was followed by Nicholson and Petropoulos (1968, 1971, 1973, 1975), who solved numerically the transport equation in several two- and three-dimensional networks. If the porous medium or pore network repeats itself periodically in space—that is, it consists of identical unit cells spanning the whole space—it can be shown (Ryan et al., 1980; Gavalas and Kim, 1981) that the problem reduces to solving the transport equation only for the unit cell.

If the interstices between the solid walls in the porous medium are considerably larger than the mean free path in the gas phase, flux expressions may also be derived following a third approach in which the gas phase is treated as a continuum. As a result, several methods developed to treat conduction in multiphase media may be used to develop flux relations and estimate effective diffusion coefficients. The problem of effective conductivity (thermal, electrical, etc.) in multiphase media dates back to the 19th century when Maxwell (1881) developed an expression for the effective conductivity of a system consisting of nonconducting, uniformly sized spheres embedded in a medium of known conductivity. Maxwell's result was later extended by Rayleigh (1892) for application to a uniform medium interrupted by cylindrical or spherical (conducting) obstacles arranged in rectangular arrays. Bruggeman (1935) investigated media with obstacles with various geometries in an attempt to improve Rayleigh's result in both two and three dimensions. For a three-dimensional dispersion of spheres the following expression was obtained for isotropic effective media:

$$(1-\epsilon)\frac{\nu-\dfrac{q_e}{q_b}}{\nu+2\dfrac{q_e}{q_b}}+\epsilon\frac{1-\dfrac{q_e}{q_b}}{1+2\dfrac{q_e}{q_b}}=0 \tag{1}$$

In Eq. 1, q_e stands for the effective conductivity, q_b is the conductivity of the medium, ϵ is the porosity, and ν is the ratio of the conductivity of the obstacles to that of the medium. Bruggeman's results were generalized by Landauer (1952)—and later by various other investigators—into the so-called effective-medium theory (EMT) when he treated each crystal in a binary crystal mixture independently, as if it were surrounded by a homogeneous medium of unknown electrical conductivity. A similar analysis was later performed by Kirkpatrick (1973) in random networks of electrical resistors in two and three dimensions. The EMT equation thus obtained relates the effective conductivity/conductance of the inhomogeneous medium/network to the distribution of conductivities/conductances of the different phases/resistors and their interconnectiveness, the latter represented by a coordination number z:

$$\int_{q,g}\frac{(q,g)-(q_e,g_e)}{(q,g)+\left(\dfrac{z}{2}-1\right)(q_e,g_e)}f[(q,g)]\,d(q,g)=0 \tag{2}$$

In Eq. 2, g denotes the conductance of a resistor in the network, and (q, g) is used to indicate q or g in this order. Observe that for a two-phase medium Eq. 2 reduces to Eq. 1 for coordination number equal to 6.

The effective-medium theory can be used in a straightforward fashion to obtain the effective diffusivity of some species in a multiphase system simply by using the diffusivity in place of conductivity q in Eq. 2 and identifying $f(g)$ with the porosity distribution density (Davis et al., 1975; Davis, 1977). If each pore in a network is treated as a resistor, Eq. 2 may also be employed to estimate the effective conductance of each pore in the network, as was done by Benzoni and Chang (1984) for a network of micropores and macropores. The relation of the effective conductance of the pores to the effective diffusivity of the medium, however, is not obvious, and Benzoni and Chang had to resort to rather arbitrary definitions of "effective" pore length and radius in order to extract the value of the effective diffusivity.

In what follows, the problem of mass transport in a class of pore networks is considered, and a procedure for estimating effective diffusivities in such structures is developed. Applications to solids with various pore size distributions follow, and the predictions of our method are compared with effective diffusivities obtained from the exact (numerical) solution of the transport equation in large networks.

Pore Network Representation of Porous Media and Effective Diffusivities

The concept of a lattice arises in physical sciences from consideration of a set of abstract objects, called atoms or sites, that are interconnected via paths called bonds. In general, a lattice is characterized by its dimensionality, its coordination number, and its microscopic topology (Dullien, 1979). We build our pore network around a lattice of uniform coordination number in the sense that the bonds of the lattice serve as axes of the pores of the network, as represented by item *f* in Figure 1. In this way, all properties of the original lattice are transferred to the pore network; thus, we can speak of pore network dimensionality and coordination number. The coordination number is equal to the average number of bonds leaving each site (Shante and Kirkpatrick, 1971), which is alternatively called "node."

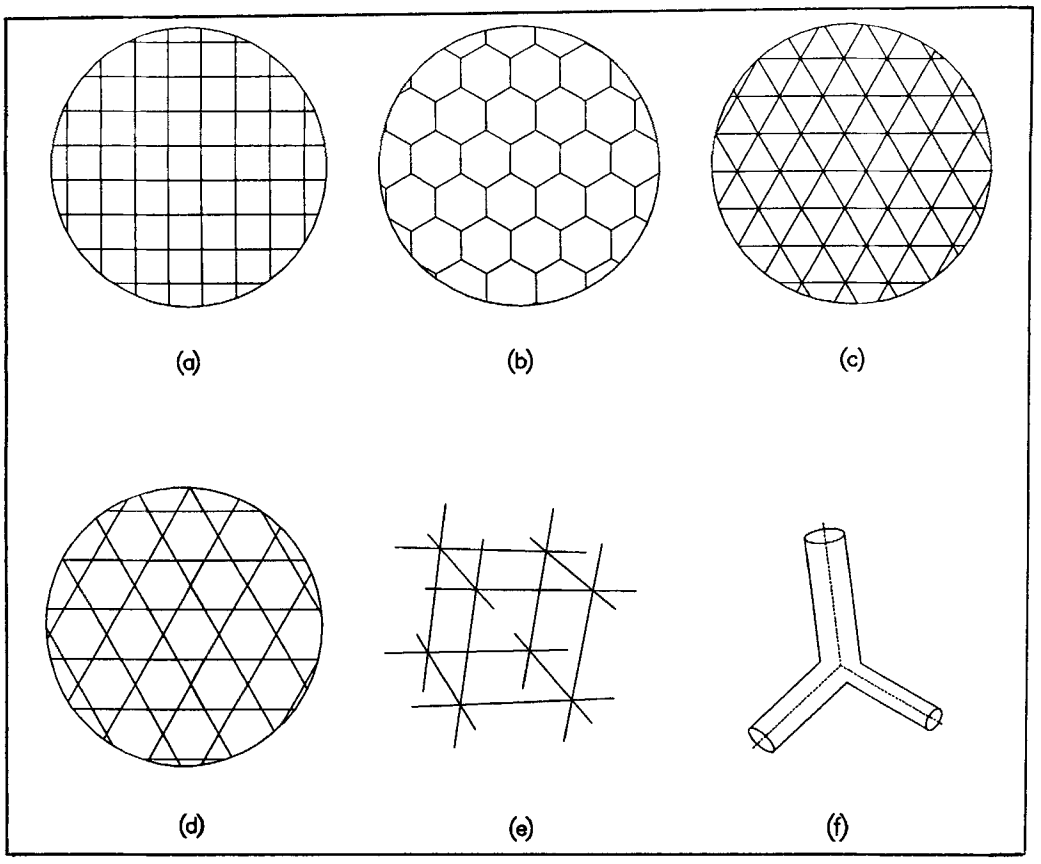

Figure 1. Lattices and pore networks.
a. Square; b. Hexagonal; c. Triangular; d. Kagomé; e. Cubic; f. Node of a pore network

Some two- and three-dimensional lattices of uniform coordination number are shown in *a–e* of Figure 1. Observe that the microscopic topology of the square and Kagomé lattices is different although their dimensionalities and coordination numbers are the same. If a two-dimensional lattice is used as skeleton of the pore network, it is understood that the porous medium is visualized as consisting of parallel layers, with the two-dimensional network embedded in each layer. The cross section of each pore segment is circular and uniform in size along the pore axis. The length of the pores is considerably larger than their radius so that flux expressions that hold for long pores can be used in each pore segment.

We describe the pore network using the distribution density $F(r, l)$ where $F(r, l)dldr$ is the number of pores per unit volume with radius in the interval $[r, r + dr]$ and length in $[l, l + dl]$. This is related to the usual porosity density function, for negligible overlap volume at the nodes, by the relation

$$\epsilon(r) = \pi r^2 \int_l lF(r, l)dl \tag{3}$$

A network of uniform pore length, l_u, can be described by the distribution density $R(r)$, with $R(r)dr$ being the number of pore segments per unit volume with radius in the interval $[r, r + dr]$, in which case

$$\epsilon(r) = R(r)\pi r^2 l_u$$

If the pore length is distributed independently of the pore size according to the distribution density $L(l)$, we may write

$$\epsilon(r) = R(r)\pi r^2 \int_l lL(l)dl \tag{4}$$

$L(l)dl$ is equal to the number fraction of pores with length in the interval $[l, l + dl]$. [We refer to $\epsilon(r)$ because it is the most frequently used distribution density for the description of a porous medium.]

For binary diffusion of species A in a pore segment identified by subscript i, we can write

$$\underline{N}_i = -D_i \nabla c_i \tag{5}$$

where D_i is the diffusion coefficient in pore i, which for small concentrations of the diffusing species can be considered independent of concentration. Under nonreactive conditions, it follows from the continuity equation for the diffusing species that $\underline{N}_i$ is constant. Using Eq. 5 we find that the rate of molar flow of A in pore i is given by

$$\dot{N}_i = -D_i \pi r_i^2 \Delta c_i / l_i \tag{6}$$

where D_i, r_i, l_i, and Δc_i are respectively the diffusion coefficient, the radius, the length, and the concentration drop between the

two ends of pore i. Introducing Eq. 6 in a material balance over a control volume containing one node only, gives the equation

$$\sum_i \frac{D_i \pi r_i^2}{l_i} \Delta c_i = 0 \tag{7}$$

where the summation involves all pores that meet at that node. Equation 7 is analogous to Kirchoff's first law for electric circuits, as it expresses a similar principle of current conservation. To complete this parallelism, we call the quantity

$$g_i = D_i \pi r_i^2 / l_i \tag{8}$$

the conductance of pore i (see also Gavalas and Kim, 1981), and assume that concentration gradients within the overlapping volume at the node can be neglected, since the size of the overlap region is much smaller than the length of the pores.

The effective diffusivity for binary diffusion in a porous medium is defined by the expression

$$\underline{N} = -D_e \nabla c \tag{9}$$

where $\underline{N}$ and ∇c are the macroscopic flux and concentration gradient, respectively. Equation 9 must be the starting point for the estimation of the effective diffusivity from experimental data or for the derivation of diffusivity expressions using some flux model for the porous medium. Notice that in writing Eq. 9 it has been tacitly assumed that vectors $\underline{N}$ and ∇c are colinear.

The macroscopic diffusion flux in the porous medium that appears in Eq. 9, can be found by averaging over a domain $\mathcal{H}$ of the three-dimensional space the contribution to the macroscopic flux of all pores lying in $\mathcal{H}$ and taking the limit that this quantity attains as domain $\mathcal{H}$ increases in size. From the definition of the macroscopic diffusion flux it follows that

$$\underline{N} = \lim_{V \to \infty} \left\{ \sum_i \frac{m_i \underline{\hat{v}}_i}{V} \right\} \tag{10}$$

In Eq. 10 the summation is taken over all pores lying in domain $\mathcal{H}$, m_i denotes the total moles of the diffusing species present in pore i, and $\underline{\hat{v}}_i$ is the average velocity of the molecules of the diffusing species in pore i. By the limiting process of Eq. 10, we mean that the characteristic length of domain $\mathcal{H}$ ($V^{1/3}$) is considerably larger than the average pore size; that is, domain $\mathcal{H}$ contains a statistically representative part of the pore network. It is understood that in writing Eq. 10 the macroscopic concentration gradient is considered constant over $\mathcal{H}$. For the pore segment indicated by index i, it can readily be shown that

$$m_i \underline{\hat{v}}_i = N_i l_i \underline{n}_i \tag{11}$$

where $\underline{n}_i$ is the unit vector parallel to the pore axis. Introducing Eq. 11 in Eq. 10 and using Eqs. 6 and 8, the expression for the macroscopic diffusion flux becomes

$$\underline{N} = -\lim_{V \to \infty} \left\{ \sum_i \frac{g_i \Delta c_i l_i}{V} \underline{n}_i \right\} \tag{12}$$

The estimation of the macroscopic flux using Eq. 12 requires knowledge of the concentration drop in each pore segment found in the control volume V, that is, the microscopic concentration field in the pore network. This can be obtained only by direct solution of the system of Eqs. 7 for a large sample of the pore network, as is done later in the section on comparison with numerical results.

Smooth field approximation

We have mentioned that the development of pore-based flux models is greatly facilitated by introducing the smooth field approximation (Jackson, 1977), that is, by assuming that the concentration gradient in a pore can be represented by the projection of the macroscopic concentration gradient on the pore axis. For a pore identified by subscript i, the smooth field approximation states that

$$\Delta c_i = l_i \underline{n}_i \cdot \nabla c \tag{13}$$

Introducing Eq. 13 in Eq. 12, we find that the macroscopic diffusion flux predicted by applying the smooth field approximation (SFA) to a pore network is given by

$$\underline{N}^S = -K \left\{ \sum_i k_i g_i l_i^2 (\underline{n}_i \underline{n}_i^T) \right\} \nabla c \tag{14}$$

where K is the number of pores per unit volume, k_i is the number fraction of pores of type i in the pore network, and the summation is taken over all types of pores present in the network.

The macroscopic diffusion flux given by Eq. 14 is not necessarily colinear with the macroscopic concentration gradient. Consequently, Eq. 14 defines, in general, an effective diffusivity tensor for the porous medium given by

$$D_e^S = K \left\{ \sum_i k_i g_i l_i^2 (\underline{n}_i \underline{n}_i^T) \right\} \tag{15}$$

which depends on the orientation of the pore network with respect to the macroscopic gradient, that is, on the unit vectors $\underline{n}_i$. Scalar effective diffusivities for isotropic porous media can be extracted from Eq. 14 if one assumes that a pore network of a certain orientation with respect to the macroscopic concentration gradient represents one of infinitely many orientational realizations of the isotropic porous medium. Consequently, the average macroscopic diffusion flux is found by averaging the result given by Eq. 14 with respect to all orientations of the pore network, i.e., with respect to all values of the unit vectors $\underline{n}_i$. Using the fact that the orientational average of the pore "tortuosity" tensor $\underline{n}_i \underline{n}_i^T$ is equal to $(1/\tau)\boldsymbol{I}$ we readily obtain from Eq. 14, using Eq. 9, that

$$D_e^S = \frac{1}{\tau} K \left\{ \sum_i k_i g_i l_i^2 \right\} \tag{16}$$

For a network of pores of uniform size, Eq. 16 becomes

$$D_e^S = \frac{1}{\tau} K \hat{g} l_u^2 \tag{17}$$

where $\hat{g}$ is equal to the number-average pore conductance. The tortuosity factor τ is equal to 3 unless the network is two-dimensional and the macroscopic concentration gradient is kept parallel to the plane defined by it. In the latter case, τ is equal to the

dimensionality of the network, i.e., 2. A similar orientational averaging process was used by Gavalas and Kim (1981) for inducing isotropicity to the periodic pore networks they studied.

Using the distribution density $F(r, l)$, Eq. 16 is written

$$D_e^S = \frac{1}{\tau} K \int_r \int_l g l^2 F^*(r, l) dl dr \tag{18}$$

Equation 18 may also be written in terms of the porosity density function, $\epsilon(r)$. Using Eqs. 3 and 8 and after some rearrangement, we obtain the expression

$$D_e^S = \frac{1}{\tau} \int_r D(r)\epsilon(r) dr \tag{19}$$

As expected, this is the expression for the effective diffusivity given by the flux models of Stewart and coworkers (Johnson and Stewart, 1965; Feng and Stewart, 1973) for small concentrations of the diffusing species in a binary mixture. If the pore length is distributed independently of the pore size, i.e., $F(r, l) = R(r)L(l)$, the expression for the effective diffusivity, Eq. 18 or 19, may also be written, using Eq. 4, in the form

$$D_e^S = \frac{1}{\tau} \epsilon \frac{\langle D(r) r^2 \rangle}{\langle r^2 \rangle} \tag{20}$$

where $\langle \cdot \rangle$ denotes the average of quantity $\cdot$ with weight function $R^*(r)$.

Unfortunately, Eq. 14 and the resulting diffusivity expressions cannot be applied to an arbitrary pore network since the smooth field approximation may violate the material balance equations at the nodes. Indeed, introducing Eq. 13 in the material balance at the nodes (Eq. 7), we get the equation

$$\sum_i g_i l_i \underline{n}_i \cdot \nabla c = 0 \tag{21}$$

which obviously does not have to be true for an arbitrary network.

Effective-medium approximation

If all nodes in the network are topologically equivalent, as is the case with networks built around the two- and three-dimensional lattices shown in Figure 1, the effective-medium theory for resistor networks (Kirkpatrick, 1973) can be used to find the effective conductance of each pore, g_e, in a uniform network that presents, approximately, the same overall resistance to diffusion as the original network. Equation 2 is now written

$$\int_g \frac{g - g_e}{g + \left(\frac{z}{2} - 1\right) g_e} f(g) dg = 0 \tag{22}$$

where $f(g)dg$ is the number of pores per unit volume of porous medium that have conductance in the interval $[g, g + dg]$. For a network of uniform pore length, the pore conductance is a single function of the pore radius, and hence $f(g)dg = R(r)dr$. For the general case of distributed pore size and pore length, independently or not, the effective medium equation for the mass transport problem in pore networks is written

$$\int_r \int_l \frac{g(r, l) - g_e}{g(r, l) + \left(\frac{z}{2} - 1\right) g_e} F(r, l) dl dr = 0 \tag{23}$$

The effective conductance that results from Eq. 22 or 23 is not directly related to the effective diffusion coefficient of the porous medium associated with the pore network considered. In their application of the effective-medium theory to a lattice of micropores and macropores, Benzoni and Chang (1984) overcame this difficulty by computing the effective diffusivity from the relation

$$D_e = g_e \hat{l} / \pi \hat{r}^2 \tag{24}$$

where $\hat{l}$ and $\hat{r}$ are the arithmetic mean values of pore length and radius. Such a relation, however, cannot be supported by any physical argument.

For a network of uniform conductance and pore length, such as the effective network of a network of pores of uniform length, Eq. 21 takes the form

$$\sum_i \underline{n}_i \cdot \nabla c = 0 \tag{25}$$

which depends only on the orientation of the pores meeting at a node. It can be easily verified that all pore networks built around the lattices shown in Figure 1 satisfy Eq. 25. Consequently, the microscopic concentration field in the effective pore network that results from networks of uniform-length pores with the topology of the lattices shown in Figure 1 can be rigorously computed by applying the smooth field assumption. In the rest of this section and in the next two sections, we will concentrate on pore networks of uniform pore length. As we shall see later in the summary section, the diffusivity expressions obtained may also be applied to networks of distributed pore length, provided that an appropriate value of l_u is used.

Since the effective network satisfies the smooth field assumption, its effective diffusivity must be given by Eq. 17, which is now written

$$D_e^{E-S} = \frac{1}{\tau} K g_e l_u^2 \tag{26}$$

Superscript E–S will be used to denote the effective diffusivities obtained from the effective-medium theory after applying the smooth field assumption (EMT-SFA procedure). The number of pores per unit volume is related to the porosity of the network by the equation

$$\epsilon = \pi K l_u \langle r^2 \rangle \tag{27}$$

For the product of the effective conductance with the pore length, on the other hand, we have that

$$g_e l_u = \pi \langle D(r) r^2 \rangle_e \tag{28}$$

where $\langle D(r)r^2 \rangle_e$ denotes the effective medium average of quantity $D(r)r^2$ with weight function $R^*(r)$. Introducing Eqs. 27 and

28 in Eq. 26 yields the expression

$$D_e^{E\text{-}S} = \frac{1}{\tau}\epsilon\frac{\langle D(r)r^2\rangle_e}{\langle r^2\rangle} \tag{29}$$

It follows from Eqs. 17, 26, and 20, 29 that

$$\frac{D_e^{E\text{-}S}}{D_e^S} = \frac{g_e}{\hat{g}} = \frac{\langle D(r)r^2\rangle_e}{\langle D(r)r^2\rangle} \tag{30}$$

For a pore network of uniform length, therefore, the deviation of the effective diffusivity based on the EMT-SFA procedure from that resulting from application of the smooth field approximation to the original network is proportional to the difference of the effective and number-average conductances, or equivalently, to the difference of the average quantities $\langle D(r)r^2\rangle e$ and $\langle D(r)r^2\rangle$. It is interesting to observe that the EMT-SFA effective diffusivity given by Eq. 29 depends on the total porosity of the pore network, the normalized form of distribution density $R(r)$, and the coordination number, but not on the pore length or the microscopic topology and dimensionality of the lattice. For instance, the effective diffusivities predicted for networks with the topology of the two-dimensional Kagomé and square lattices, Figure 1, and of the three-dimensional diamond lattice are the same for given ϵ and $R^*(r)$.

Applications

We consider a network of uniform-length pores that is built around the regular cubic lattice shown in Figure 1e. Using Eqs. 17 and 26 and the fact that $K = 3/l_u^3$, we have that

$$D_e^{E\text{-}S} = \frac{g_e}{l_u} \tag{31}$$

$$D_e^S = \frac{\hat{g}}{l_u} \tag{32}$$

It must be pointed out, however, that direct application of Eq. 14 to the cubic network would lead to the same result since—as can easily be shown by considering the single-pore "tortuosity" tensor in polar coordinates—the regular cubic network is isotropic. This observation also applies to all two-dimensional networks of Figure 1, although for two-dimensional diffusion. Comparison of Eq. 31 with the diffusivity expression proposed by Benzoni and Chang (1984), Eq. 24, clearly shows that their procedure overestimates the effective diffusivity of the porous medium. The ratio of the diffusivities predicted by Eqs. 31 and 24 for a network of uniform-length pores is equal to $\pi\hat{r}^2/l_u^2$, and consequently the predictions of Eqs. 31 and 24 approach each other only if $\hat{r}$ and l_u become comparable. In such a case, however, the analysis on which the development of Eqs. 31 and 24 was based is no longer valid since Eq. 6 does not hold for short cylinders and the overlap volume at the nodes cannot be neglected.

An expression for the diffusion coefficient in a single pore is needed for applications. For binary diffusion of small concentrations of species A in a long pore segment, we have that the diffusivity in the pore is given by

$$D = \frac{D_K}{1 + \dfrac{D_K}{\mathcal{D}}} = \frac{Qr}{1 + \dfrac{Qr}{\mathcal{D}}}$$

where D_K is the Knudsen diffusivity in the pore, $\mathcal{D}$ is the bulk diffusion coefficient, and Q is the proportionality constant between D_K and pore radius. The pore conductance is then written, using Eq. 8, as

$$g = \frac{Q\pi}{l}\frac{r^3}{1 + \dfrac{Qr}{\mathcal{D}}} \tag{33}$$

Treating $Q/\mathcal{D}$ as a parameter, the whole transition regime between the limiting cases of bulk and Knudsen diffusion control can be investigated.

We will first examine what happens for a discrete multimodal distribution of pore size with porosity density

$$\epsilon(r) = \sum_{i=1}^{p}\epsilon_i\delta(r - r_i)$$

The number density for the pore conductances then has the form

$$f(g) = \sum_{i=1}^{p} f_i\delta(g - g_i)$$

where g is given by Eq. 33. It can readily be shown that

$$f_i = \frac{\epsilon_i}{\pi r_i^2 l_u} \tag{34}$$

while Eq. 22 reduces to a p-term summation

$$\sum_{i=1}^{p} f_i\frac{g_i - g_e}{g_i + \left(\dfrac{z}{2} - 1\right)g_e} = 0 \tag{35}$$

For the special case of a bimodal pore size distribution ($p = 2$) applied to a cubic pore network ($z = 6$), Eq. 40 reduces further to a quadratic equation, whose solution is

$$g_e = \frac{(2\alpha - 1)g_1 + (2 - \alpha)g_2}{4(1 + \alpha)} + \frac{1}{4(1 + \alpha)}\{[(2\alpha - 1)g_1 + (\alpha - 2)g_2]^2 + 36\alpha g_1 g_2\}^{1/2} \tag{36}$$

with

$$\alpha = \frac{f_1}{f_2} = \left(\frac{\epsilon_1}{\epsilon_2}\right)\left(\frac{r_2}{r_1}\right)^2 \tag{37}$$

The variation of the effective diffusivity ratio $D_e^{E\text{-}S}/D_e^S$, Eq. 30, with the porosity ratio (ϵ_1/ϵ_2) for a discrete bimodal pore system arranged in a regular cubic network is shown in Figure 2 for $r_1/r_2 = 10$. We observe that the effective diffusion coefficients obtained by direct application of the smooth field approximation to the original network are significantly larger than those resulting from the effective pore network, by more than one order of magnitude in some cases. The difference between the two effective diffusivities increases as we move from the bulk diffusion regime towards the Knudsen regime. The reason for this behavior of the results lies in the fact that the ratio of the two types of

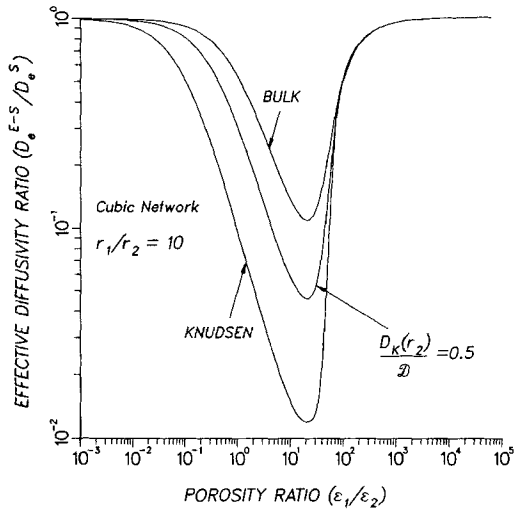

Figure 2. Dependence of D_e^{E-S}/D_e^S ratio on porosity ratio of a bimodal pore system.

conductances that exist in the network changes from 10^2 for $r_1/r_2 = 10$ in the bulk diffusion regime to 10^3 in the Knudsen regime, Eq. 33. Similar conclusions are also derived from Figure 3, which presents the dependence of D_e^{E-S}/D_e^S for Knudsen diffusion on the pore size ratio of the bimodal system. It is again observed that the SFA predictions are considerably higher than those of the effective-medium theory, except for the two monodisperse limits $\epsilon_1/\epsilon_2 = 0$ and $\epsilon_1/\epsilon_2 \to \infty$ where the difference between the two diffusivities becomes identically zero.

It is not surprising that the effective-medium theory always predicts lower effective diffusivities. After some rearrangement Eq. 35 may be written in the form

$$\frac{\sum_{i=1}^{p} f_i}{\frac{z}{2} g_e} = \sum_{i=1}^{p} \frac{f_i}{g_i + \left(\frac{z}{2} - 1\right) g_e} \tag{38}$$

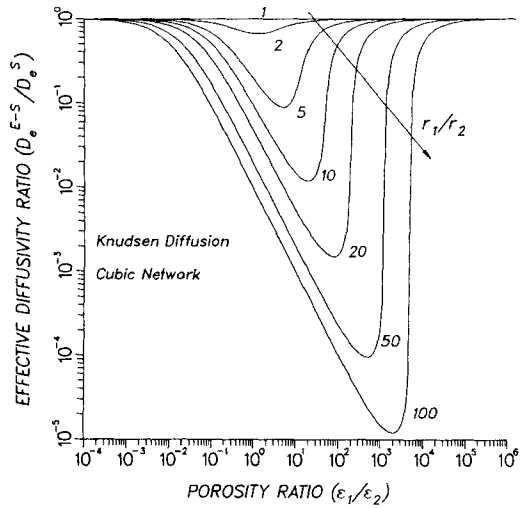

Figure 3. Variation of ratio of EMT-SFA and SFA effective diffusivities for Knudsen diffusion with porosity ratio and pore size ratio of a bimodal pore system.

For coordination number $z = 2$ one readily realizes that the effective-medium theory, as expressed by Eq. 38, treats the diffusional resistances of the pore network as if they were in series. On the other hand, if we divide Eq. 35 by $(z/2) - 1$ and take the limit as $z \to \infty$, we find that the effective-medium conductance is equal to number-average conductance $\hat{g}$, that is, the diffusional resistances are added in parallel. For other coordination numbers an intermediate situation results. However, the effective diffusivity predicted by applying the smooth field approximation to the original network is always based on the number-average conductance, Eq. 17, and consequently it is higher than that predicted by the effective-medium theory.

More results for the diffusivity ratio D_e^{E-S}/D_e^S of a cubic network are shown in Figures 4, 5, and 6 for continuous distributions of pore size or pore conductance. Figure 4 presents results for a normal pore size distribution with density function

$$R(r) = A \exp\left[-\frac{(r - r_m)^2}{2\sigma^2}\right] H(r)$$

where A is a constant and the Heaviside function $H(r)$ is employed to exclude negative pore sizes. As in the case of a discrete bimodal distribution, it is seen that the smooth field approximation predicts larger effective diffusivities if it is directly applied to the original network. As expected, the difference of the EMT and SFA predictions increases as the distribution of pore size becomes broader, i.e., as the normalized standard deviation, σ/r_m, increases. The predictions of the smooth field approximation deviate from the effective-medium result more in the Knudsen diffusion regime since the pore conductance given by Eq. 33 varies over a wider range for Knudsen diffusion.

A similar trend is exhibited by the curves of Figure 5, where the pore size distribution is taken to be uniform over the range $[r_*, r^*]$, i.e., with distribution density $R(r) = A/(r^* - r_*)$. For this density function, the integration in Eq. 22 can be carried out analytically to give an algebraic equation, expressed in terms of transcendental functions, which is then solved numerically to obtain the value of g_e. The diffusivity or conductance ratio

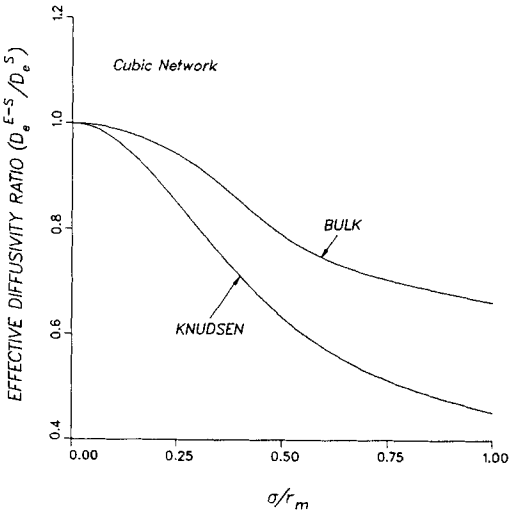

Figure 4. Dependence of effective diffusivity ratio on standard deviation, σ/r_m, of a normal distribution density of pore size, $R(r)$.

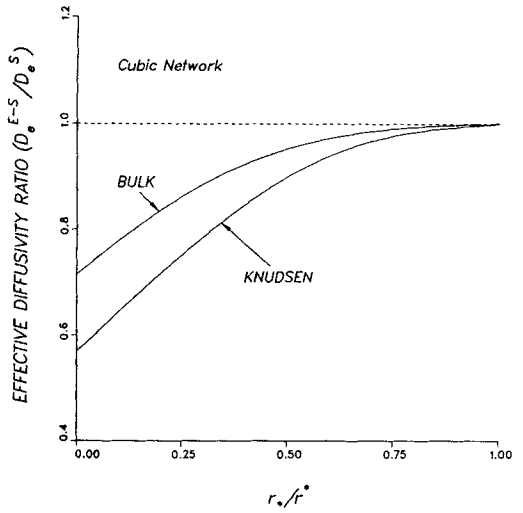

Figure 5. Dependence of effective diffusivity ratio on ratio of limits of pore size range, r_*/r^*, for a solid with uniform number distribution density of pore size, $R(r)$.

(D_e^{E-S}/D_e^S or $g_e/\hat{g}$) depends only on the ratio of the limits of the pore size range (r_*/r^*) that is used as abscissa in Figure 5. Once more it is seen that the predictions of the two methods approach each other in the vicinity of the monodisperse limit only (i.e., $r_*/r^* = 1$). Notice that for $r_*/r^* = 0$ the diffusivity ratio of Figure 5 approaches a finite value. This is not, however, the case if the porosity of the pore network is assumed to be distributed uniformly over $[r_*, r^*]$, i.e., $\epsilon(r) = A/(r^* - r_*)$. Results for this case are shown in Figure 6, where it is observed that as $r_*/r^* \to 0$, the diffusivity ratio, D_e^{E-S}/D_e^S, also approaches zero. This behavior is due to the fact that the diffusivity predicted by the EMT-SFA procedure becomes zero as $r_*/r^* \to 0$. As can be shown, the integrals of the density functions $f(g)$ and $R(r)$ approach infinity for the above form of $\epsilon(r)$ as g and r approach zero.

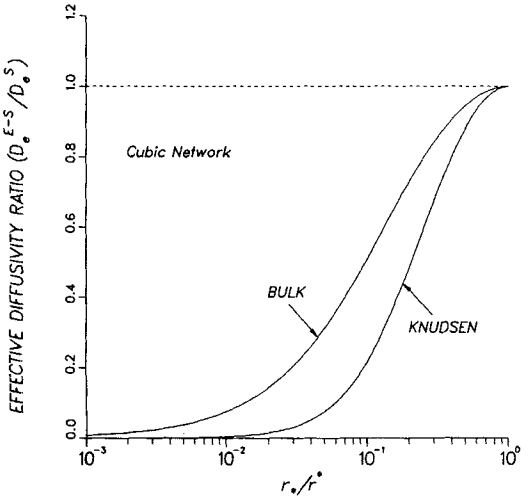

Figure 6. Dependence of effective diffusivity ratio on ratio of limits of pore size range, r_*/r^*, for a solid with uniform porosity density function, $\epsilon(r)$.

Comparison with Numerical Results

In this section the effective diffusivity in square and cubic networks is computed "exactly" through probabilistic modeling of the porous medium using Monte Carlo simulation procedures, and the results are compared with the predictions of the SFA and EMT-SFA approximations. If the smooth field assumption is not invoked in the analysis of the original network, the microscopic concentration field that is needed for the computation of the macroscopic flux $\underline{N}$ using Eq. 12 can be found only by directly solving the equations that describe mass transport in the pore network. Application of Eq. 12 requires knowledge of the microscopic concentration field in a domain $\mathcal{H}$ of the porous medium, of volume V, whose characteristic size ($V^{1/d}$) is much larger than the average pore length. The mass transport problem in domain $\mathcal{H}$ is described by the nodal balances, Eq. 7, at the interior nodes complemented by a set of boundary conditions induced by the macroscopic concentration gradient. For a cubic network, we consider a cubic domain whose bounding planes are parallel to the faces of the unit cells of the lattice and intersect the lattice at nodal positions. Equation 7 is then written for all interior nodes, and appropriate boundary conditions are applied to nodes lying on the boundary of the cubic domain.

Some remarks regarding the choice of boundary conditions are in order here. Let us consider a system of rectangular coordinates x, y, and z positioned in such a way that its axes are respectively perpendicular to the three pairs of parallel faces of the cubic domain. Let $\underline{n}_x$, $\underline{n}_y$, and $\underline{n}_z$ denote the unit vectors along the axes of the Cartesian coordinate system. The simplest choice of boundary conditions results if the macroscopic concentration gradient is considered perpendicular to a pair of parallel bounding planes, for instance, those parallel to the yz plane. The nodal concentrations at these two planes are then set equal to c_0 and $c_0 + \Delta c_x$, respectively, where the concentration difference Δc_x is related to the macroscopic concentration gradient by the relation $\Delta c_x = a\nabla c \cdot \underline{n}_x$, where a is the side of the cubic domain. Since there is no net diffusion in directions that are normal to the macroscopic concentration gradient, the side boundary planes, i.e., those parallel to the x-axis, are simply assumed to be impervious to diffusion; that is, the molar flow in pores ending at sites lying on the side planes is set equal to zero. Another alternative for the boundary conditions applied to nodes lying on the side planes is to assume that the pore network extends to infinity in directions perpendicular to the macroscopic gradient in the sense that the cubic domain $\mathcal{H}$ serves as its unit cell; that is, translation by distance a along the y or z axis leaves the network invariant. The concentrations at nodes that are separated by distance a in the directions parallel to the y or z axis are therefore equal, and periodic (cyclic) boundary conditions apply to points lying on opposing faces of domain $\mathcal{H}$. Such boundary conditions were used by Kirkpatrick (1973) in his numerical investigation of the percolation properties of three- and two-dimensional lattices (cubic and square).

The fact that the macroscopic concentration gradient is taken perpendicular to a pair of faces of the cubic domain $\mathcal{H}$ does not limit the generality of the results because of the isotropicity of the cubic lattice. If no assumption about the direction of the macroscopic concentration gradient is made, we may consider that the pore network extends to infinity in all directions, that is, translation by a along the x, y, or z direction leaves the network invariant. The boundary conditions are then obtained by utilizing the observation that the solid is now characterized by a

periodic structure in all three directions with domain $\mathcal{H}$ serving as its unit cell. Consequently, the concentration difference between pairs of points that are separated by distance a in the direction parallel to the unit vector $\underline{n}_x$, $\underline{n}_y$ or $\underline{n}_z$ satisfies the relation (Gavalas and Kim, 1981) $\Delta c_{x,y,z} = a\nabla c \cdot \underline{n}_{x,y,z}$, where x, y, z denotes x, y, or z in this order. The set of algebraic equations (nodal balances and boundary conditions) that results if the above procedure is followed is linearly dependent, and its solution requires that the value of the concentration at one nodal point of $\mathcal{H}$ be specified (Gavalas and Kim).

Similar procedures are followed in setting up the numerical simulation equations for the square network. However, diffusion now occurs in two dimensions, and only one "slice" of the porous medium (with the two-dimensional network embedded in it) is considered. The linear algebraic system that results in both cases (cubic and square) with any choice of boundary conditions has the general form

$$\underline{A}\underline{c} = \underline{b} \tag{39}$$

where $\underline{c}$ is the vector of nodal concentrations. The structure of matrix $\underline{A}$ is sparse and similar to that of matrices arising in finite-difference schemes. Most elements of $\underline{b}$ are also zero, with the exception of those corresponding to sites located at the bounding planes. The linear systems of algebraic equations, eq. 39, were solved using standard iterative procedures developed for elliptic differential equations discretized by finite differences in two or three dimensions (Lapidus and Pinder, 1982). Specifically, overrelaxation led to marked acceleration of the convergence of the Gauss-Seidel iterative scheme and made it possible to handle large samples of the porous medium (for instance, 200 × 200 for the square and 40 × 40 × 40 for the cubic network) within reasonable computational time. The nodal concentrations were then used to compute the macroscopic flux vector, and thence the effective diffusivity, by use of Eqs. 12 and 9.

The assignment of radii, and hence of conductances, to the pores lying in $\mathcal{H}$ was accomplished through random sampling from a prescribed distribution of pore size, as expressed by the density function $R(r)$, using standard procedures in the literature (Cashwell and Everett, 1959; Bird, 1976). For sufficiently large sample sizes, the differences among the results obtained with different boundary conditions proved to be negligible. However, it must be mentioned that the third set of boundary conditions, with domain $\mathcal{H}$ serving as the unit cell of the porous medium in all three directions, appeared to give results that were more close to the "exact" effective diffusivity (i.e., the value obtained for very large samples). For a given pore network, a number of different realizations of domain $\mathcal{H}$ were employed in our computations to eliminate the possibility of working with nonrandom sequences.

Results for pore networks with discrete bimodal distribution of pore size are shown in Figure 7 for a three-dimensional cubic network. The results are presented in terms of the ratios of the effective diffusivities predicted by the SFA and EMT-SFA approximations to the numerically computed value, which are plotted as functions of the porosity ratio of the discrete bimodal system ($r_1/r_2 = 10$). It is seen in Figure 7 that the EMT-SFA predictions almost coincide with the "exact" results over a wide range of porosity ratio, ϵ_1/ϵ_2, both for Knudsen and bulk diffusion. On the other hand, the SFA effective diffusivity is always larger than the numerically computed value, which it approaches only at the two unimodal limits ($\epsilon_1/\epsilon_2 \to 0$ and $\epsilon_1/\epsilon_2 \to \infty$).

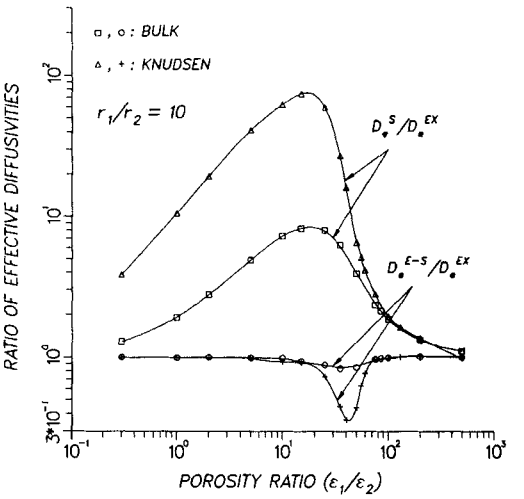

Figure 7. Comparison of EMT-SFA and SFA approximations with simulation results for a cubic pore network with discrete bimodal distribution of pore size.

The existing differences between the numerically computed effective diffusivity and that given by the EMT-SFA approximation over a relatively narrow range of porosity ratio are not surprising. They relate to the well-known fact (Kirkpatrick, 1971, 1973) that the effective-medium theory does not provide a satisfactory approximation of the effective conductance of a lattice of conducting and nonconducting bonds ($g_2 = 0$) close to its percolation threshold, that is, close to the value of the number ratio of conducting and nonconducting bonds ($\alpha = f_1/f_2$, according to our notation) below which the conducting bonds exist only in the form of isolated, finite clusters (Kirkpatrick, 1971, 1973). As can be found using Eq. 35 for $p = 2$ and $g_2 = 0$, the percolation threshold predicted by the effective-medium theory for a network of coordination number z is equal to $2/z$. This gives a percolation threshold of 0.33 for a cubic lattice, while the exact value is about 0.25 (Shante and Kirkpatrick, 1971). However, both types of bonds (pores) considered in the network of Figure 7 are conducting. Thus, as the percolation threshold is neared by decreasing the f_1/f_2 ratio (or equivalently, ϵ_1/ϵ_2), diffusion through the smaller pores becomes dominant and the effective diffusivity that is computed numerically or predicted by the effective-medium theory goes through a drastic decrease approaching the value corresponding to a unimodal pore system, of small pores only. As can be clearly seen in Figure 8, this happens at a higher ϵ_1/ϵ_2 value for the effective-medium theory—since the percolation threshold is also larger—leading to quantitative differences between the numerical results and the EMT-SFA approximation.

Similar behavior is exhibited by the results obtained for two-dimensional (square) pore networks, which are shown in Figure 9. However, the observed differences between the exact diffusivity and that predicted by the EMT-SFA procedure are markedly smaller than those seen in Figure 7 for cubic networks. The

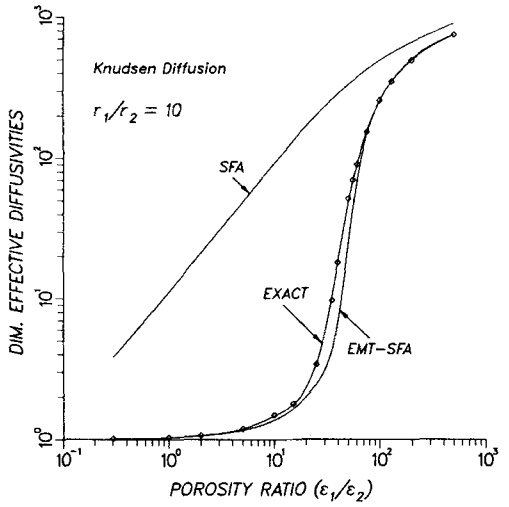

Figure 8. Variation of "exact," EMT-SFA, and SFA effective diffusivities with porosity ratio for the pore network of Figure 7.

reason is that the effective-medium theory predicts exactly the percolation threshold of a square lattice, which is equal to 0.5 (Shante and Kirkpatrick, 1971), and consequently the observed differences mainly arise from the different slopes of the "exact" and EMT-SFA effective diffusivity vs. α curves in the vicinity of the percolation threshold.

Comparison of the results for cubic and square networks, Figures 7 and 9, reveals that the predictions of the SFA approximation are worse for the square network. This is in accord with our observation that as the coordination number of the network increases, parallel combination of the resistances in the network starts to dominate, leading eventually (as $z \to \infty$) to negligible differences between the "exact" result and the SFA value. Another interesting observation is that the maxima in the D_e^S/D_e^{EX} ratio of Figures 7 and 9 are located close to the corresponding percolation thresholds. (In terms of the porosity ratio of the pore network, the percolation threshold of the cubic lattice is located at $\epsilon_1/\epsilon_2 = 25$, while the corresponding value for the square lattice is 50.)

The observed differences in Figures 7 and 9 between the "exact" effective diffusivity and the two approximations increase as Knudsen diffusion becomes the dominant form of mass transport mechanism in the pores (compare with Figure 2). This is expected since moving from the bulk to the Knudsen diffusion regime leads to a tenfold increase in the ratio of the two types of resistances present in the pore network (for $r_1/r_2 = 10$). Still, even in the Knudsen regime and for the cubic network, the EMT-SFA approximation should be considered satisfactory as it never becomes worse than 30%, while the SFA procedure overestimates the effective diffusivity by more than two orders of magnitude. In view of the above observations, the EMT-SFA approximation is expected to perform considerably better for narrower bimodal or multimodal distributions of pore size. This should also be the case for continuous distributions of pore size, which allow for smooth variation of the diffusional resistance with the pore size. Results for a pore network with uniform distribution of pore size [$R(r) = A/(r^* - r_*)$] are presented in Figure 10, where the ratios of EMT-SFA and SFA effective diffusivities to the "exact" diffusivities are plotted as functions of the ratio of the limits of the pore size range, r_*/r^* (compare with Figure 5). Indeed, we see there that the effective diffusivity based on the EMT-SFA approximation almost coincides with the exact result over the whole range of possible r_*/r^* values. This is not, however, true for the diffusivity obtained using the SFA procedure, which again is considerably higher than the "exact" value.

Summary and Further Remarks

The mass transport problem in random-pore networks of a certain class was investigated, and a procedure for estimating effective diffusivities in porous media characterized by such porous structures was formulated. The pore networks considered consist of long, straight, cylindrical capillaries of distributed radius arranged around the bonds of a two- or three-dimensional

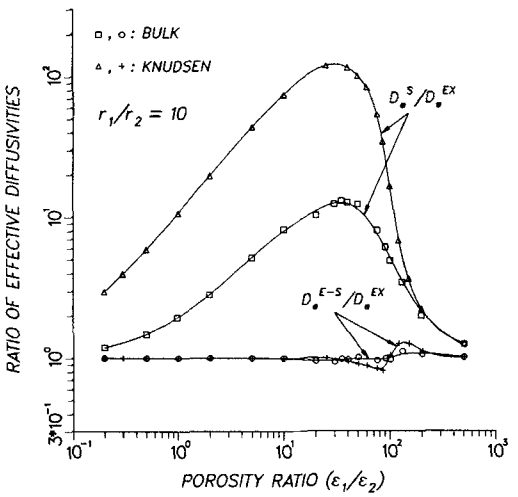

Figure 9. Comparison of EMT-SFA and SFA approximations with simulation results for a square pore network with discrete bimodal distribution of pore size.

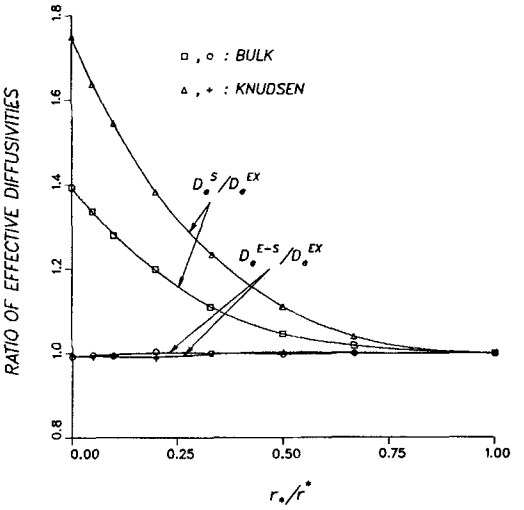

Figure 10. Comparison of EMT-SFA and SFA approximations with simulation results for a cubic pore network with uniform number distribution density of pore size, $R(r)$.

lattice of uniform coordination number in such a way that the bonds of the lattice serve as axes of the capillaries. (A two-dimensional network is considered to be embedded in a slice of the porous medium.) The effective-medium theory, as it has been developed for resistor networks, is used to obtain an effective conductance for the network, which is then used to determine the effective diffusivity starting from first physical principles and utilizing the observation that a network of pores of uniform conductance satisfies the smooth field approximation.

Comparison of the effective diffusivity obtained through the above procedure with the "exact" value determined through Monte Carlo simulation of the random-pore network revealed that the EMT-SFA procedure provides an excellent shortcut method for estimating effective diffusivities in random-pore networks of uniform coordination number. Extensive computer simulations for pore networks with discrete bimodal pore size distribution showed that the EMT-SFA predictions deviate significantly from the "exact" result only as the ratio of the populations of large and small pores approaches the percolation threshold of the lattice.

Direct application of the smooth field approximation to the original random-pore network violates the mass balance equations at the nodes of the network and leads to overestimation of the effective diffusion coefficient, by more than one order of magnitude in some cases. This is due to the fact that the smooth field approximation always assumes that the resistances to mass transport in the network are combined in parallel, while in actuality a situation that is intermediate to parallel and series combinations of the diffusion resistances obtains. The differences of the SFA predictions from the "exact" and EMT-SFA result diminish as the coordination number of the network increases and the distribution of pore size becomes narrower.

The flux relations and the attendant effective diffusivity expressions that are obtained by direct application of the smooth field approximation to the original network, Eqs. 14 and 19, hold for uniform as well as distributed length networks. However, the EMT-SFA procedure developed in second Section for deriving flux expressions and estimating effective diffusivities is applicable to pore networks of uniform length only. For the general case of a random network of distributed pore size and pore length, described by the distribution density $F(r, l)$, Eq. 23 may be used to obtain the value of the effective conductance of the network, but Eq. 26 applies to networks of uniform-length pores only.

We can overcome this difficulty by observing that the set of Eqs. 7 that provides, together with appropriate boundary conditions, the microscopic concentration field in the network depends only on the distribution of conductances in the network and on the number of nodes per unit volume. In other words, if some pores in the network are shortened or lengthened, the vector of nodal concentrations in domain $\mathcal{H}$, which serves as a representative of the whole pore network, does not change provided that the radii of the pores are decreased or increased accordingly so that their conductances remain the same. We can therefore assume that the original pore network is equivalent, with respect to mass transfer, to a new network of uniformly sized pores with the same distribution of conductances, the same coordination number, and the same number of mass transport channels (pores) per unit volume. If the new network is not isotropic, it is understood that the various expressions derived for it are orientationally averaged. Equation 26 can then be applied to the uniform-length network to yield EMT-SFA expressions for the original network. The length of the pores of the equivalent network is needed for such an application. If the normalized form, $F^*(r, l)$, of the distribution density $F(r, l)$ is known, the number of pores per unit volume of the original network can be obtained from the expression

$$K = \epsilon \Big/ \int_l \int_r \pi r^2 l F^*(r, l)\, dr dl \tag{40}$$

On the other hand, for a uniform-length network of known microscopic topology and coordination number, we have that

$$K = \text{function}(z, \text{topology}, l_u) \tag{41}$$

The righthand sides of Eqs. 40 and 41 are set equal to each other, and the resulting expression is then solved for l_u. It follows from Eqs. 23, 26, 40, and 41 that the effective diffusivity (EMT-SFA approximation) of a pore network of given $F^*(r, l)$ and ϵ depends on the coordination number and the microscopic topology of the associated lattice only. Thus, if the effective diffusion coefficient is also known (from mass transport experiments, for instance), the above equations may be used to determine the coordination number and the microscopic topology of the pore network.

Acknowledgment

Acknowledgment is made to the Donors of the Petroleum Research Fund, administered by the American Chemical Society, for partial support of this research. This research was also supported in part by a grant from the U.S. Department of Energy.

Notation

a = side of cubic domain used in simulation computations
A = proportionality constant
c = concentration of diffusing species
d = dimensionality of network
D = diffusion coefficient
$\mathcal{D}$ = bulk diffusivity
D_K = Knudsen diffusivity
$\underline{\underline{D}}$ = diffusivity tensor
$f(g)dg$ = number of pores (bonds) per unit volume with conductance in range $[g, g + dg]$
f_i = number of pores (bonds) per unit volume with conductance g_i in a network with discrete distribution of conductance or pore size
$F(r, l)drdl$ = number of pores per unit volume with size in range $[r, r + dr]$ and length in range $[l, l + dl]$
g = conductance of a pore (bond)
$\underline{\underline{I}}$ = unit matrix
k_i = number fraction of pores of type i
K = total number of pores per unit volume
l = length of a pore
l_u = pore length in a network of pores of uniform length
$L(l)dl$ = number fraction of pores with length in range $[l, l + dl]$
$\underline{n}_i$ = unit vector parallel to the axis of pore i
$\underline{n}_{x,y,z}$ = unit vector parallel to the x, y, z axis of a Cartesian coordinate system
$\underline{N}$ = macroscopic diffusion flux
$\underline{N}_i$ = diffusion flux in pore i
$\dot{N}_i$ = rate of molar flow in pore i
Q = proportionality constant
r = pore radius
r_m = most probable pore radius in a normal distribution of pore size

r_* = lower limit of pore size range
r^* = upper limit of pore size range
$R(r)dr$ = number of pores per unit volume with radius in range $[r, r + dr]$
V = volume
z = coordination number

Greek letters

α = population ratio in a discrete bimodal pore system
Δc = concentration difference between the two ends of a pore
∇c = macroscopic concentration gradient
∇c_i = concentration gradient in pore i
ϵ = porosity
$\epsilon(r)dr$ = porosity of pores with radius in range $[r, r + dr]$
ϵ_i = porosity of pores of radius r_i in a network with discrete distribution of pore size
σ = standard deviation of a normal distribution

Subscripts

e = effective quantities
i = quantities referring to a pore of type i or to the ith pore size of a discrete pore size distribution

Superscripts

$\hat{}$ = average quantities
E–S = effective diffusivities or quantities obtained from effective-medium theory after applying smooth field assumption
EX = "exact" effective diffusivities computed numerically
S = effective diffusivities or quantities based on smooth field approximation

Literature Cited

Benzoni, J., and H. C. Chang, "Effective Diffusion in Bidisperse Media—An Effective-Medium Approach," *Chem. Eng. Sci.*, **39,** 161 (1984).

Bird, G. A., *Molecular Gas Dynamics,* Clarendon, Oxford (1976).

Bruggeman, D. A. G., "Berechnung verschiedener physikalisher konstanten von heterogenen substanzen," *Ann. Physic.*, **24,** 636 (1935).

Cashwell, E. D., and C. J. Everett, *A Practical Manual on the Monte Carlo Method for Random Walk Problems,* Int. Tracts Computer Sci. Technol. and Their Application, v. 1, Pergamon, New York (1959).

Cunningham, R. E., and R. J. J. Williams, *Diffusion in Gases and Porous Media,* Plenum, New York (1980).

Davis, H. T., "The Effective-Medium Theory of Diffusion in Composite Media," *J. Am. Ceram. Soc.*, **60,** 499 (1977).

Davis, H. T., L. R. Valencourt, and C. E. Johnson, "Transport Processes in Composite Media," *J. Amer. Ceram. Soc.*, **58,** 446 (1975).

Dullien, F. A. L., *Porous Media—Fluid Transport and Pore Structure,* Academic Press, New York (1979).

Feng, C., and W. E. Stewart, "Practical Models for Isothermal Diffusion and Flow of Gases in Porous Solids," *AIChE J.*, **12,** 143 (1973).

Gavalas, G. R., and S. Kim, "Periodic Capillary Models of Diffusion in Porous Solids," *Chem. Eng. Sci.*, **36,** 1111 (1981).

Jackson, R., *Transport in Porous Catalysts,* Elsevier, Amsterdam (1977).

Johnson, M. F. L., and W. E. Stewart, "Pore Structure and Gaseous Diffusion in Solid Catalysts," *J. Catal.*, **4,** 248 (1965).

Kirkpatrick, S., "Classical Transport in Disordered Media: Scaling and Effective-Medium Theories," *Phys. Rev. Lett.*, **27,** 1722 (1971).

———, "Percolation and Conduction," *Rev. Mod. Phys.*, **45,** 574 (1973).

Landauer, R., "The Electrical Resistance of Binary Metallic Mixtures," *J. Appl. Phys.*, **23,** 779 (1952).

Lapidus, L., and G. F. Pinder, *Numerical Solution of Partial Differential Equations in Science and Engineering,* Wiley, New York (1982).

Mason, E. A., and A. P. Malinauskas, *Gas Transport in Porous Media: The Dusty-gas Model,* Elsevier, New York (1983).

Mason, E. A., A. P. Malinauskas, and R. B. Evans III, "Flow and Diffusion of Gases in Porous Media," *J. Chem. Phys.*, **46,** 3199 (1967).

Maxwell, J. C., *A Treatise on Electricity and Magnetism,* Clarendon, Oxford (1881).

Nicholson, D., and J. H. Petropoulos, "Capillary Models for Porous Media. I: Two-phase Flow in a Serial Model," *J. Phys. D: Appl. Phys.*, **1,** 1379 (1968).

———, "Capillary Models for Porous Media. III: Two-phase Flow in a Three-Dimensional Network with Gaussian Radius Distribution," *J. Phys. D: Appl. Phys.*, **4,** 181 (1971).

———, "Capillary Models for Porous Media. IV: Flow Properties of Parallel and Serial Capillary Models with Various Radius Distributions," *J. Phys. D: Appl. Phys.*, **6,** 1737 (1973).

———, "Capillary Models for Porous Media. V: Flow Properties of Random Networks with Various Radius Distributions," *J. Phys. D: Appl. Phys.*, **8,** 1430 (1975).

Rayleigh, J. W., "On the Influence of Obstacles Arranged in Rectangular Order Upon the Properties of a Medium," *Phil. Mag.*, **34,** 481 (1892).

Ryan, D., R. G. Carbonell, and S. Whitaker, "Effective Diffusivities for Catalyst Pellets under Reactive Conditions," *Chem. Eng. Sci.*, **35,** 10 (1980).

Shante, V. K. S., and S. Kirkpatrick, "An Introduction to Percolation Theory," *Adv. Phys.*, **20,** 325 (1971).

Sotirchos, S. V., and V. N. Burganos, "Intraparticle Diffusion and Char Combustion," *Chem. Eng. Sci.*, **41,** 1599 (1986).

Sotirchos, S. V., and H. C. Yu, "Mathematical Modeling of Gas-Solid Reactions with Solid Product," *Chem. Eng. Sci.*, **40,** 2039 (1985).

van Brakel, J., "Pore-space Models for Transport Phenomena in Porous Media. Review and Evaluation with Special Emphasis on Capillary Liquid Transport," *Powder Technol.*, **11,** 205 (1975).

Manuscript received July 9, 1986, and revision received Mar. 11, 1987.